IEEE Access
Multidisciplinary | Rapid Review | Open Access Journal

Received 25 June 2022, accepted 11 July 2022, date of publication 18 July 2022, date of current version 25 July 2022.

Digital Object Identifier 10.1109/ACCESS.2022.3192124

RESEARCH ARTICLE

Vehicle State Estimation Based on Multidimensional Information Fusion

DUANYANG TIAN[1,2], LIQIANG JIN[1], ZHIHUI ZHANG[2], AND HAO LI[1]
[1]State Key Laboratory of Automotive Simulation and Control, Jilin University, Changchun 130022, China
[2]Key Laboratory of Bionic Engineering of Ministry of Education, Jilin University, Changchun 130022, China

Corresponding author: Duanyang Tian (tiandy0702@163.com)

This work was supported by the National Key Research and Development Program of China under Grant 2021YFB2500007.

ABSTRACT As the core input parameters of various control systems, the real-time and accurate acquisition of reference speed, mass and road slope is the key factor to improve the performance of intelligent vehicle dynamics control. Therefore, the parameter estimation method based on multi-dimensional information fusion is proposed in this paper. A comprehensive evaluation of wheel dynamics state is realized by information fusion, which is quantified in terms of wheel speed credibility. Then the calculated dynamic speed and auxiliary speed are weighted coupled to achieve accurate estimation of reference speed, which avoids the influence of unstable wheels. Similarly, the method to calculate the confidence factor of mass estimation is established in order to screen the vehicle state suitable for estimation. And the online estimation of mass is realized based on recursive least square method. Meanwhile, the road slope estimation algorithm based on interactive multiple model has been designed, which achieves the weighted fusion of Kalman filter observer based on kinematics and unscented Kalman filter observer based on dynamics. Finally, the road tests were carried out on representative working conditions. The maximum error between the actual speed and the reference speed does not exceed 0.68m/s. The relative error of mass estimation is not more than 1.95%, and the absolute error of slope estimation is less than 1.84%, which proves that the proposed estimation algorithm has high comprehensive performance. More importantly, it is not limited to specific working conditions, which means a great significance for the development of intelligent vehicles.

INDEX TERMS Vehicle state estimation, multi-information fusion, reference speed, steady state evaluation.

I. INTRODUCTION

Vehicle driving state estimation not only serves dynamics control [1], but also provides important help for intelligent driving decision [2]. Its accuracy and real-time performance directly affect the actual effect of system functions, and even determine the stability and safety of the vehicle [3], [4]. However, how to realize the recognition of vehicle dynamics state change in all scenarios is still the core problem of dynamics control function industrialization. In addition, the new electric drive [5] or X-by-wire platform has the characteristics of faster response and more accurate execution [6], which also puts forward higher requirements for vehicle state identification algorithm. Estimation based on traditional single sensor information cannot meet the above requirements, so it is necessary to use information fusion technology [7], [8] to obtain more detailed and accurate conclusions from multi-source information of the single vehicle and even from internet of vehicles [9], [10].

The reference speed is one of the most basic and core input signals in various control systems [11], [12]. Because it directly influences the calculation of key parameters such as wheel slip rate [13], [14], slip angle [15], [16] and road excitation [17], and then has an impact on dynamics control [18], [19] and ADAS [20], [21]. Especially, for driverless vehicles committed to the development of safer and more intelligent L3 level and above, accurate reference speed estimation can further ensure that the vehicle achieves desired path tracking in any situation [22]. So some scholars use in-vehicle camera [23] and develop a variety of image processing methods [24] to achieve speed estimation. However, considering the actual working environment and cost issues,

The associate editor coordinating the review of this manuscript and approving it for publication was Shaohua Wan.

special sensors such as optical cameras, are not suitable for promotion in products [25], [26]. Reference speed estimation algorithms can be divided into two kinds from the principle [27]: one is based on wheel speed and basic measurement signals such as longitudinal acceleration for calculation [28], e.g., the maximum wheel speed method, the slope method, the integrated method, etc. [29], but the methods have poor stability, accuracy and limited adaptability to the ESC system; The other is based on vehicle dynamics model [30],but the algorithm is greatly affected by the accuracy of the vehicle and tire model, which is less adaptive to different road [31]. On this basis, some scholars take the lead in using the method of information fusion [32], [33] for speed estimation. In some studies [34], GPS and other sensor information are introduced. Using kinematics and dynamics methods, GPS information correction in slope and other working conditions is realized. There are also scholars [35] who use multi-sensor information to build high-precision vehicle models, but the real-performance of these methods and the accuracy of the model need to be further considered. But these studies [36]–[39] still haven't completely gotten rid of the limitations of specific scenarios, and the actual performance under complex working conditions cannot be known.

In addition, vehicle mass and road slope are also very important to dynamics control functions [40]. And due to high coupling relationship [41], their estimation methods are also closely related. For mass estimation, it is usually realized based Newton's second law and with the help of recursive least square (RLS) method [42], [43], Kalman filter (KF) [44], [45] and so on [43]. However, in practice, due to driver inputs and environmental changes, the state of vehicles may change drastically, which is not conducive to mass identification. Therefore, the core problem is how to describe the stable state of the vehicle quantitatively. And the principle of slope estimation can be divided into two aspects: kinematics and dynamics. The kinematics method [47], [48] requires accurate longitudinal velocity and acceleration as the basis, but it is greatly affected by vehicle state changes. The dynamics method relies on the vehicle model, but it is obviously affected by high frequency noise. Therefore, how to realize the fusion calculation of the two methods to achieve accurate estimation is the key problem that needs to be solved urgently. Meanwhile, many studies [49] realized mass and slope estimation based on the vehicle speed signal by EMS (Engine Manage System) or other systems, but the update frequency and property of such signal cannot be guaranteed, which will also affect the estimation results. It can be seen from the existing research and the development trend of vehicle control technology, on the basis of ensuring the accuracy of the estimation results, shortening the update cycle to meet the needs of the electric drive platform and improving the adaptability of the algorithm in complex scenarios are the research directions of vehicle state estimation algorithms in the future.

In order to meet the performance requirements of intelligent vehicles on related state parameters and solve the problem that the existing algorithm has poor adaptability in realistic comprehensive working conditions, this paper proposes the estimation method of reference speed, mass and slope based on the idea of multi-information fusion. The choice of different algorithms is mainly to consider the characteristics of the estimated parameters and the requirements of the control function. For the reference speed, the method of calculating the wheel speed credibility based on multi-dimensional information comprehensive evaluation is proposed, in which the wheel speed credibility is a quantitative representation of the stable state of wheel dynamics. Then the corresponding wheel speed signal is weighted according to each wheel speed credibility, and the reference speed is obtained by combining the longitudinal acceleration signal. Similarly, in order to estimate the mass under suitable working conditions, the calculation method of confidence factor is proposed, and the RLS is used to get the final estimation result. Then, the fusion estimation of KF kinematics slope observer and UKF(Unscented Kalman Filter) [50] dynamics slope observer is realized by using IMM(Interactive Multiple Model) [51]. Finally, the road tests are carried out under representative working conditions, the maximum estimation error of reference speed is less than 0.68m/s, the mass estimation error is not more than 1.95%, and the road slope estimation error is less than 1.84%, which has important practical significance for the development of intelligent vehicle control functions.

II. REFERENCE SPEED ESTIMATION BASED ON WHEEL SPEED CREDIBILITY

A. WHEEL SPEED SIGNAL PROCESSING

Wheel speed signal is as the basic signal of reference speed estimation, its quality and processing method directly affects the accuracy of estimation results [52]. Fig.1 shows the analysis process of the wheel speed signal and the captured wheel speed pulse signal. In a fixed sample period T_s, the time between the last falling (or rising) edge of the previous cycle and the last falling (or rising) edge of the current cycle is ΔT_1 (ΔT_2), and the corresponding number of edges is N_1 (N_2). The wheel speed v_{rad} is calculated as Eq. (1).

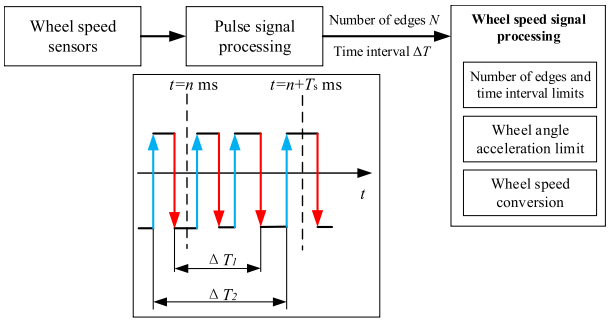

FIGURE 1. Wheel speed signal acquisition and processing.

In reality, the wheel speed sensor as the weak current system [53], its signal is subject to a lot of interference [54].

Therefore, the maximum number of edges $N_{\max}$ acquired in a single period should be limited first, as shown in Eq. (2).

$$v_{\text{rad}} = N_i \cdot 2\pi \cdot r_{\text{w}}/(n_{\text{teeth}} \cdot \Delta T_i) \quad i = 1, 2 \tag{1}$$

$$N_{\max} = V_{\max} \cdot T_{\text{s}} \cdot n_{\text{teeth}}/(2\pi \cdot r_{\text{w}}) \tag{2}$$

where $V_{\max}$ is the maximum vehicle speed, n_{teeth} is the number of wheel speed sensor teeth and r_{w} denotes the wheel radius. The maximum limit of the time interval should correspond to the number of pulse edges acquired, the independent limitation is meaningless. In addition, the outlier or wild point in the wheel speed signal should be judged and removed by the angular acceleration. The calibration of the maximum angular acceleration needs to take it into account that the physical limits of the actual wheel, and the possible noise part of the wheel speed signal.

After the necessary limitation, since the reference speed represents the longitudinal absolute speed of the vehicle, the lateral motion component and longitudinal slip component in the wheel speed signal should be removed. In the process of conventional driving, the wheel slip rate does not exceed 2% generally. As the slip rate has a linear relationship with the road adhesion coefficient within the range of small slip rate, the slope is defined as K_{ci}.

$$K_{ci} = \frac{\mu_i}{sl_i} i = 1, 2, 3, 4 \tag{3}$$

where μ_i denotes the available adhesion coefficient, sl_i is the wheel slip rate. Taking the rear axle center as the reference point, the wheel speed along the longitudinal vehicle body can be expressed as.

$$v'_{\text{wRi}} = \frac{(v_{\text{wi}} \cdot K_{\text{ci}}/(K_{\text{ci}} + \mu_i) \mp \omega \cdot L \cdot sin\delta_w)}{\cos\delta_{\text{w}}} \mp \omega \cdot B/2 \quad i = 1, 2 \tag{4}$$

$$v'_{\text{wRi}} = (v_{\text{wi}} \cdot K_{\text{ci}}/(K_{\text{ci}} + \mu_i) \mp \omega \cdot B/2 \quad i = 3, 4 \tag{5}$$

where v'_{wRi} represents the rolling longitudinal velocity of the wheel converted to the reference point, v_{wi} is the wheel speed after the maximum limit, ω denotes yaw rate, L is the axle base, B is the wheelbase and δ_{w} is the wheel steering angle, i = 1,2,3,4 respectively denotes left front wheel, right front wheel, left rear wheel and right rear wheel. In order to verify the effect of correction, the slalom test was carried out in steady state, as shown in Fig. 2. Four wheel speed signals converted to the reference point are basically equal, which is in line with expectations.

B. WHEEL SPEED CREDIBILITY CALCULATION BASED ON MULTI-DIMENSIONAL INFORMATION

When the vehicle drives stably, corrected wheel speed is approximately equal to the actual speed. But when the state of the wheel is unstable, especially when the active control function is enable, the wheel speed changes dramatically. It must be accurately identified to reduce the interference to the reference speed calculation. The comprehensive evaluation method of wheel dynamics stable state is realized by judging multi-dimensional information based on fuzzy

FIGURE 2. Comparison of wheel speeds before and after correction.

rules with information fusion technology, as shown in Fig. 3. Multi-dimensional information includes wheel longitudinal force F_{bi}, wheel speed v'_{wRi}, reference speed v_{ref}, longitudinal acceleration a_x and the number of wheels under ABS (Anti-lock Braking System) control N_{ABS}, etc. The fuzzy rules are divided into stable unit and state unit considering that the wheel state features are different under different driving states of vehicles. The stable unit is concerned with the change of force, which is most relevant to the wheel stability. The state unit main focuses on the relationship between wheel speed and vehicle speed. As the wheel speed is most prone to drastic fluctuations in the deceleration state (anti-lock braking, active booster braking), so it is further divided into three conditions.

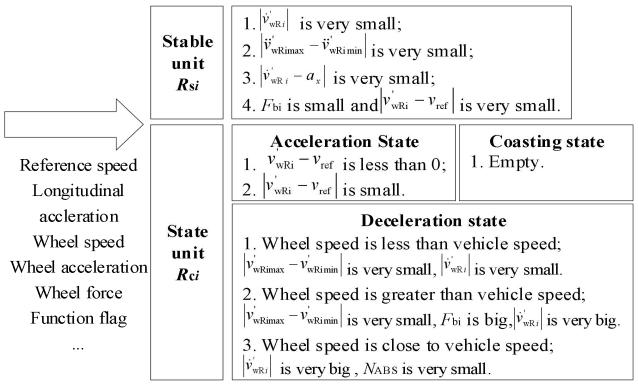

FIGURE 3. Fuzzy rules corresponding to high wheel speed credibility.

The above fuzzy rules are made based on the wheel dynamics theory and road test experience. The advantage of the algorithm is that the robustness and applicability can be effectively improved in comprehensive scenario. But it needs a lot of test data as support, and the workload is usually large. After data processing, the domain of each input signal and parameter range are set in the following table.

Except for the three cases in the deceleration conditions, the logic relationship between the rules within each unit should be ''and'', that is, taking a small operation, so as to calculate R_{si}, and R_{ci}. Finally the wheel speed credibility factor is output as Eq. (6), ranging from 0 to 1, where 1 indicates that the wheel dynamics state is extremely stable.

$$R_{\text{w}i} = \min(R_{\text{s}i}, R_{\text{c}i}), i = 1, 2, 3, 4 \tag{6}$$

TABLE 1. Parameters of the fuzzy subsets.

Input signal \ Fuzzy subsets	ST	S	M	L	LT
$\lvert\dot{v}'_{\mathrm{wR}i}\rvert$	0~4	3~9	8~11	10~19	17~
$\lvert v'_{\mathrm{wR}i\max} - v'_{\mathrm{wR}i\min}\rvert$	0~0.2	0.1~0.3	0.25~1.5	1.25~2.5	2~
$\lvert\dot{v}'_{\mathrm{wR}i\max} - \dot{v}'_{\mathrm{wR}i\min}\rvert$	0~2	1~5	4 ~ 6.4	6~7.5	7~
$\lvert\ddot{v}'_{\mathrm{wR}i\max} - \ddot{v}'_{\mathrm{wR}i\min}\rvert$	0~5	3~15	10~80	75~200	175~
$\lvert v'_{\mathrm{wR}i} - v_{\mathrm{ref}}\rvert$	0~0.1	0.07~0.2	0.15~0.9	0.8~1	1~
$\lvert\dot{v}'_{\mathrm{wR}i} - a_x\rvert$	0~0.2	0.1~0.45	0.3~1.65	1.5~2.2	2~
F_{bi}	0~100	50~200	150~600	500~900	800~
N_{ABS}	0	1	2	3	4

C. PRINCIPLE OF REFERENCE SPEED ESTIMATION

On the one hand, the wheel speed credibility represents the comprehensive evaluation result of multi-dimensional information on wheel stable state; On the other hand, it also represents the proximity between the corresponding wheel speed and the real vehicle speed. Therefore, the reference speed estimation principle is designed as shown in Fig. 4. First, the auxiliary vehicle speed v_{x1} is calculated by using the reference speed of the previous cycle v_{refk1} and the estimated longitudinal acceleration a_x of the current cycle. Then, each wheel speed is weighted by the corresponding wheel speed credibility and averaged to get the dynamic vehicle speed v_{x2}. Finally, reference speed is the dynamic coupling result of v_{x1} and v_{x2} as shown in Eq. (13).

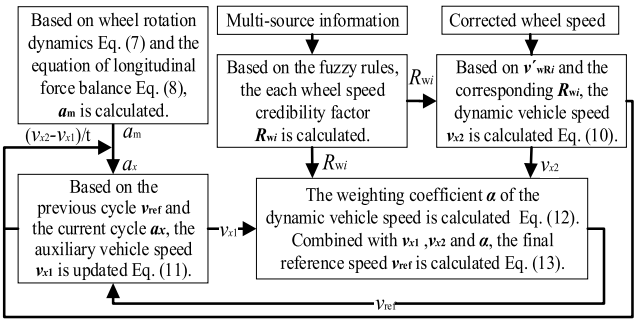

FIGURE 4. Architecture of the reference speed estimation algorithm.

Additionally, Eq. (9) is used to correct the estimated value of vehicle longitudinal acceleration to compensate for the impact of road slope. The slope estimation results are not directly used in order to avoid the system instability caused by the mutual iteration of the two estimation algorithms. The weight coefficient α of v_{x1} and v_{x2} is calculated by each wheel speed credibility, as shown in Eq. (10). Because when only a single wheel is stable, the algorithm can still output an accurate result, the range of f_1 is [0.5,1]. It should be noted that the method of v_{x1} and v_{x2} dynamic coupling is adopted to ensure that the reference speed can still be estimated accurately by the auxiliary vehicle speed (acceleration iteration) when the force on all wheels change dramatically. At the same time, the problem of using acceleration iteration for a long time is avoided, because in practice, continuous iteration will produce cumulative errors which are difficult to be eliminated. The following are the relevant equations involved in the above.

$$F_{bi} = [J_w \cdot \dot{v}'_{wRi}/r_w - T_{Di} + T_{Bi}]/r_w,\ i = 1, 2, 3, 4 \quad (7)$$

$$a_m = [\sum_{i=1}^{4} (F_{bi}) - F_w]/m_v \quad (8)$$

$$a_x = a_m + (v_{x2} - v_{x1})/t \quad (9)$$

$$v_{x1} = v_{\mathrm{refk1}} + a_x \cdot t \quad (10)$$

$$v_{x2} = 0.25 \sum_{i=1}^{4} (R_{wi} \cdot v'_{wRi}) \quad (11)$$

$$\alpha = f_1 \cdot \max(R_{wi}) + (1 - f_1) \cdot 0.25 \sum_{i=1}^{4} (R_{wi}) \quad (12)$$

$$v_{ref} = \alpha \cdot (v_{x2} - v_{x1}) + v_{x1} \quad (13)$$

where J_w is the wheel moment of inertia, T_{Di} denotes wheel drive moment, T_{Bi} denotes wheel brake moment, a_m indicates the theoretical longitudinal acceleration, F_w is air resistance, t denotes the running period. T_{Di} and T_{Bi} are respectively from the drive and brake system, which need to be filtered based on the actual signal characteristics to ensure the stability of the estimated acceleration value.

It should be added that when the active function does not fail, it is not usual for all wheels to over slip or lock. However, if all wheel speed fail, the wheel speed credibility will be very low. In this case, the proposed algorithm will estimate based on slope method to ensure the minimal estimation error. The fuzzy rules of the proposed multi-information fusion reference speed estimation algorithm are based on a large number of test data. Compared with the traditional estimation algorithm, the concept of wheel speed credibility is proposed as the intermediate value to reduce the difficulty of making fuzzy rules. By weighting dynamic speed and auxiliary speed, the proposed algorithm is not limited to specific working conditions, and can accurately estimate vehicle speed in actual comprehensive scenarios.

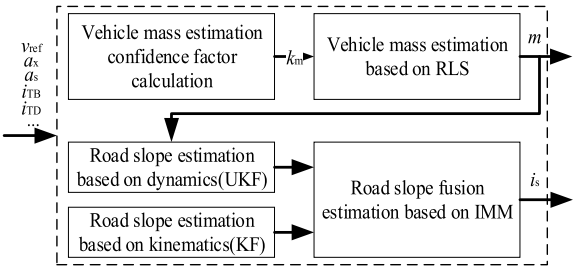

FIGURE 5. Estimation algorithm architecture.

III. VEHICLE MASS AND ROAD SLOPE ESTIMATION BASED ON MULTI-INFORMATION FUSION

The architecture of estimation algorithm is shown in Figure 5. Information fusion technology can make use of multi-source information to obtain more accurate judgment of vehicle real state, which helps to avoid the influence of

vehicle unstable state on relevant estimation results. Hence the vehicle mass estimation confidence factor based on multi-information fusion is proposed and mass estimation is realized based on RLS. Because of the coupling relationship between vehicle mass estimation and road slope estimation, the result of mass estimation is input to the slope estimation algorithm. The slope estimation based on dynamics needs mass as input, and its stability is poor. The slope estimation algorithm based on kinematics needs acceleration as input, but the estimation accuracy is poor because the vehicle attitude is not considered. Therefore, IMM algorithm is designed to realize the weighting of the two methods, which effectively solves the above problems.

A. VEHICLE MASS ESTIMATION CONFIDENCE FACTOR CALCULATION

In transient scenarios with drastic changes, the actual state estimation results will be distorted due to signal fluctuations. Therefore, it is necessary to evaluate the stable state of the vehicle comprehensively and effectively. Fuzzy rules are adopted, and reference speed v_{ref}, longitudinal acceleration a_x, relative driving and braking torque coefficient i_{TD}, i_{TB} are selected as input signals. The relative torque coefficient is the ratio of the actual output torque to the maximum torque, which can expand the applicable scope of fuzzy rules and reduce the calibration workload. The specific fuzzy rules are set as follows.

R1: If v_{ref} is M and $|a_x|$ is S and i_{TD} is not L and i_{TB} is not L, then L.

R2: If v_{ref} is not L and $|a_x|$ is not L and i_{TD} is S and i_{TB} is S, then L.

R3: If v_{ref} is not L and $|a_x|$ is not L and i_{TD} is not L and i_{TB} is M, then M.

R4: If v_{ref} is not L and $|a_x|$ is M and i_{TD} is not L and i_{TB} is not L, then M.

R5: If v_{ref} is S or $|a_x|$ is L or i_{TD} is L or i_{TB} is L, then S.

Fuzzy subsets are shown in the table below. The output is the mass estimation confidence factor k_{m}, its domain is [0,1]. S is [0, 0.6], M is [0.5, 0.75], L is [0.7, 1].

TABLE 2. Parameters of the fuzzy subsets.

Input signal \ Fuzzy subsets	S	M	L
V_{ref}	0~6	5~25	20~
$\|a_x\|$	0~3	2~5	4~
i_{TD}	0~0.3	0.2~0.6	0.5 ~
i_{TB}	0~0.2	0.15~0.4	0.35~

The fuzzy rules mentioned are based on the dynamics theory. Besides, gear shifting and active function intervention need to be considered. In these two cases, the wheel force changes dramatically and cannot be accurately calculated, so the confidence factor k_{m} should be directly set as 0.

B. VEHICLE MASS ESTIMATION BASED ON RLS

The complete longitudinal force balance equation of the vehicle is shown in Eq. (14).

$$F_{\text{d}} = F_{\text{w}} + F_{\text{f}} + F_{\text{s}} + F_{\text{j}} \tag{14}$$

where F_{d} is vehicle driving force, F_{f} is rolling resistance, F_{s} denotes slope resistance, F_{j} indicates acceleration resistance. The above equation is sorted according to whether the variable includes mass or not, as shown in Eq. (15). F_{res} represents the driving force minus the resistance unrelated to mass, which is called the equivalent driving force.

$$F_{\text{res}} = F_{\text{d}} - F_{\text{w}} = F_{\text{f}} + F_{\text{s}} + F_{\text{j}} = m(gf + a_{\text{s}}) \tag{15}$$

where f denotes the coefficient of rolling resistance, a_{s} is acceleration sensor signal, which includes slope resistance and acceleration resistance. Thus, the above equation can be further expressed as Eq. (16), where a_{res} is the equivalent acceleration.

$$F_{\text{res}} = m \cdot a_{\text{res}} \tag{16}$$

As mass is a slow-changing parameter, the requirement of real-time performance is not high. Therefore, cyclic iteration can be adopted to reduce the estimation error, and considering that the least square method will significantly increase the amount of calculation over time, RLS is finally adopted in this paper. Although RLS has the disadvantage of not being able to fit nonlinear data, it can be seen from Eq. (16) that it is suitable for solving this problem. So the mass estimation model is established. a_{res} is the input φ, F_{res} is the system output z, and m is the model parameter θ to be identified. The recursion process is as follows.

$$\hat{\theta}(k) = \hat{\theta}(k-1) + \gamma(k)[z(k) - \varphi^T(k)\hat{\theta}(k-1)] \tag{17}$$

$$\gamma(k) = P(k-1)\varphi(k)[\varphi^T(k)P(k-1)\varphi(k) + \lambda(k)]^{-1} \tag{18}$$

$$P(k) = [I - \gamma(k)\varphi^T(k)]P(k-1)/\lambda(k) \tag{19}$$

where $\gamma(k)$ is the gain at time k, $P(k)$ denotes the covariance matrix, $\lambda(k)$ represents the time-varying forgetting factor. In order to output a accurate and stable result, the mass estimation based on RLS is performed only when the calculated mass estimation confidence factor k_{m} is greater than the threshold T_{k}. And considering that mass is a slowly changing state parameter, it does not need to be updated continuously. The estimation flow chart is designed as shown in Fig. 6. f_{c} denotes the convergence flag. When the covariance P_{c} is less than the set threshold T_{p}, f_{c} is enabled, and the result of mass estimation is updated; Otherwise, the last estimation result is output. After the estimate converges, the mass estimation is restarted only when the parking time t_{p} exceeds the threshold T_{t} and the door or boot is opened (f_{d} =1).

C. ROAD SLOPE ESTIMATION BASED ON IMM

In order to realize the coupling estimation of slope based on kinematics and dynamics principles using IMM, two estimation methods should be established respectively first. Considering that the road slope is usually continuous, the state of

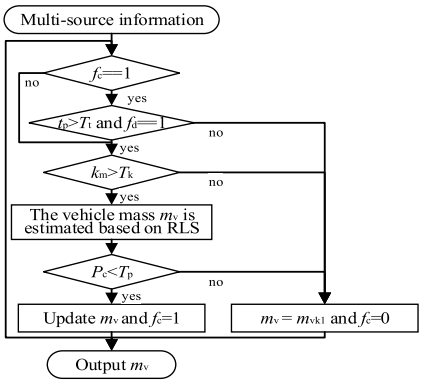

FIGURE 6. Flow chart of the vehicle mass estimation algorithm.

the previous moment will have an impact on the results of the next moment. So RLS is not suitable for solving this problem. It is well known that KF is a special case of least square method, and it has good smoothness to meet the requirements of the estimated parameters. However, because KF has the same limitation that it can only accurately estimate the linear model, so UKF is also needed for dynamics estimation method.

1) ROAD SLOPE ESTIMATION BASED ON KINEMATICS

Vehicle acceleration sensor signal contains information of speed change and slope. Considering road slope changes slowly relative to vehicle dynamic state, it can be assumed that it derivative is approximately 0.

$$\begin{cases} \dot{v}_{\text{ref}}(t) = a_{\text{sen}} = a_{\text{x}} - \text{g}\cdot i_{\text{s}} \\ \dot{i}(\text{t}) = 0 \end{cases} \tag{20}$$

where i_{s} denotes slope. By discretizing the above equation, the state space equation at time t can be shown.

$$\begin{cases} x_t = A \cdot x_{t-1} + B \cdot u_t + n_t \\ z_t = H \cdot x_t + m_t \end{cases} \tag{21}$$

where $A = \begin{bmatrix} 1 & -\text{g}\cdot\Delta t \\ 0 & 1 \end{bmatrix}$, $B = \begin{bmatrix} \Delta t \\ 0 \end{bmatrix}$, $H = \begin{bmatrix} 1 \\ 0 \end{bmatrix}^{\text{T}}$, $x_t = \begin{bmatrix} v_{\text{ref}} \\ i \end{bmatrix}$, $u_t = a_x$, $z_t = v_{\text{ref}}$, n_t is process noise, m_t denotes measurement noise, where n_t and m_t are mutually independent Gaussian white noise, and corresponding covariance matrix is Q, R. KF algorithm is used to estimate slope i, as shown below.

$$\begin{cases} \hat{x}_t^- = A\hat{x}_{t-1} + Bu_t \\ P_t^- = AP_{t-1}A^{\text{T}} + Q \\ K_t = P_{\text{t}}^- H^{\text{T}}(HP_t^- H^{\text{T}} + R)^{-1} \\ \hat{x}_t = \hat{x}_t^- + K_t(z_t - H\hat{x}_t^-) \\ P_t = (I - K_t H)P_t^- \end{cases} \tag{22}$$

where $\hat{x}_t^-$ and $\hat{x}_{t-1}$ represent the prior and posterior state estimates at different times respectively, P_t^- and P_{t-1} indicate the prior and posterior estimates of the covariance matrix respectively, K_t is the Kalman gain.

2) ROAD SLOPE ESTIMATION BASED ON DYNAMICS

Vehicle is a complex nonlinear system. Based on Eq. (14), the longitudinal dynamic equation can be expressed as.

$$m\dot{v} = F_{\text{d}} - F_{\text{j}} - F_{\text{w}} - F_{\text{f}} - F_{\text{s}} \tag{23}$$

$$F_{\text{s}} = mg\cdot i_{\text{s}} \tag{24}$$

It can be seen that the slope estimation algorithm based on dynamics is affected by vehicle mass, so the mass estimates is taken as the input. The nonlinear state equation of the system is established as follows.

$$\begin{cases} x_t = f(x_{t-1}, n_t) \\ z_t = H \cdot x_t + m_t \end{cases} \tag{25}$$

Therefore the linear Kalman filter algorithm is no longer applicable. And the UKF uses Unscented Transformation(UT) to sample state values, and its core is to find a Gaussian distribution that is approximate to the real distribution, so the calculation accuracy of the UKF is higher. The basic steps are as follows:

(1) $2n+1$ sigma points are constructed through UT, where $n = 2$, and corresponding weights ω are obtained at the same time. The method is as follows.

$$\begin{cases} x^{(0)} = \bar{x}, e = 0 \\ x^{(0)} = \bar{x} + (\sqrt{(n+\sigma)P})_e, e = 1 \sim n \\ x^{(0)} = \bar{x} - (\sqrt{(n+\sigma)P})_e, e = n+1-2n \end{cases} \tag{26}$$

$$\begin{cases} \omega_{\text{a}}^{(0)} = \dfrac{\sigma}{n+\sigma} \\ \omega_{\text{c}}^{(0)} = \dfrac{\sigma}{n+\sigma}(1-\alpha^2+\beta) \\ \omega_{\text{a}}^{(0)} = \omega_{\text{c}}^{(0)} = \dfrac{\sigma}{2(n+\sigma)}, e = 1-2n \end{cases} \tag{27}$$

$$\sigma\alpha^2(n+\kappa) - n \tag{28}$$

where $\bar{x}$ is the average of the state vector, P denotes the covariance of the state vector, a and c represent mean and covariance respectively, σ indicates the scale parameter, and smaller it is, the closer the sigma point is to the mean of the states. α, β, κ are optional parameters.

(2) According to Eq. (26), (27), a set of sampling points and corresponding weights ω are obtained to calculate the prediction estimates $\hat{x}_t^-$ and covariance matrix P_t^-.

$$\begin{cases} \hat{x}_t^- = \sum_{e=0}^{2n} (\omega_{\text{a}}^{(e)} \hat{x}_{t-1}^{(e)}) \\ P_t^- = \sum_{e=0}^{2n} \omega_{\text{b}}^{(e)} [\hat{x}_t^- - \hat{x}_{t-1}^{(e)}][\hat{x}_t^- - \hat{x}_{t-1}^{(e)}]^{\text{T}} + Q \end{cases} \tag{29}$$

(3) Based on the one-step prediction results, the set of sigma points is mapped to the new set of sigma points $\hat{x}_t^{(e)}$.

(4) The new set of sigma points $\hat{x}_t^{(e)}$ is weighted to predict the predicted mean $\bar{z}_t$ and covariance matrices $P_{z_t z_t}$.

$$\begin{cases} \bar{z}_t = \sum_{e=0}^{2n} (\omega_{\text{a}}^{(e)} z_t^{(e)}) \\ P_{z_t z_t} = \sum_{e=0}^{2n} \omega_{\text{b}}^{(e)} [z_t^{(e)} - \bar{z}_t][z_t^{(e)} - \bar{z}_t]^{\text{T}} + R \end{cases} \tag{30}$$

(5) The cross-covariance and the Kalman gain of UKF can be expressed as.

$$\begin{cases} P_{x_t z_t} = \sum_{e=0}^{2n} \omega_{\mathrm{b}}^{(e)} [x_t^{(e)} - \bar{z}_{\mathrm{t}}][x_t^{(e)} - \bar{z}_t]^{\mathrm{T}} \\ K_t = P_{x_t z_t} \cdot P_{z_t z_t}^{-1} \end{cases} \tag{31}$$

(6) The system state estimates $\hat{x}_t$ and covariance P_t are calculated as Eq. (32).

$$\begin{cases} \hat{x}_t = \hat{x}_t^- + K_t(z_t - H\hat{x}_t^-) \\ P_t = P_t^- - K_{\mathrm{t}} P_{z_t z_t} K_t^{\mathrm{T}} \end{cases} \tag{32}$$

3) ROAD SLOPE FUSION ESTIMATION BASED ON IMM

As mentioned in the introduction, there are some problems in slope estimation independently based on kinematics or dynamics. Therefore, in order to achieve accurate estimation in all working conditions, the interactive multi-model method is used to fuse the two models established above. The basic principle is to adjust the weight of different models to adapt to current state of the vehicle, automatically reduce the error interference in different environment, so as to keep the minimal tracking error of the output results. First, the prediction probability c_j of model j and mixed probability P_{mij} from model i to j are as follows. j represents model number, where 1 is based on the kinematics model and 2 is based on the dynamics model.

$$c_j = \sum_{i=1}^{2} P_{ij} P_i(t-1) \tag{33}$$

$$P_{\mathrm{m}ij}(t-1|t-1) = P_{ij} P_i(t-1)/c_j \tag{34}$$

where P_{ij} is the transition probability from model i to j, $P_i(t\text{-}1)$ denotes the probability of model i at time t-1. The mixed state estimation and mixed covariance estimation of model j are shown in Eq. (35), (36).

$$\hat{x}_{0j}(t-1|t-1) = \sum_{i=1}^{2} P_{ij} \hat{x}_i(t-1|t-1) \tag{35}$$

$$\begin{aligned} P_{0j}(t-1|t-1) = \sum_{i=1}^{2} P_{ij} \{ & P_i(t-1|t-1) \\ & [\hat{x}_i(t-1|t-1) - \hat{x}_{0j}(t-1|t-1)] \cdot \\ & [\hat{x}_i(t-1|t-1) - \hat{x}_{0j}(t-1|t-1)]^T \} \end{aligned} \tag{36}$$

where $\hat{x}_i(t-1|t-1)$ and $P_i(t-1|t-1)$ indicate the target state estimation and covariance matrix at time t-1. Then, KF and UKF are carried out for the two models respectively in order to realize parameter updating. The likelihood function is used to update the model probability, and the likelihood function of model j is expressed as.

$$\Lambda_j(t) = \frac{\exp[-v_j^{\mathrm{T}} S_j^{-1}(t) v_j/2]}{(2\pi)^{n/2} |S_j(t)|^{1/2}} \tag{37}$$

$$v_j(t) = Z(t) - H(t)\hat{x}_j(t|t-1) \tag{38}$$

$$S_j(t) = H(t) P_j(t|t-1) H(t)^{\mathrm{T}} + R(t) \tag{39}$$

The probability of model j is shown in Eq. (40).

$$P_j(t) = \Lambda_j(t) \cdot c_j/\eta \tag{40}$$

$$\eta = \sum_{j=1}^{2} \Lambda_j(t) c_j \tag{41}$$

Finally, the estimation results of the two models are weighted coupled based on the model probability to obtain the road slope estimation results.

$$\hat{x}(t|t) = \sum_{j=1}^{2} P_j(t) \hat{x}_j(t|t) \tag{42}$$

IV. REFERENCE SPEED ROAD TESTS VALIDATION

The reference speed estimation algorithm based on multi-dimensional information fusion proposed in this paper can achieve accurate vehicle speed estimation under realistic comprehensive conditions. In order to verify its actual performance, the low adhesion test condition is selected. Because in this case, the wheel dynamics state is relatively more unstable and more difficult to estimate. Meanwhile, in order to verify the real-time performance of the algorithm and quantify the estimation accuracy, VBOX III data acquisition system of the Racelogic company is used. The GPS magnetic antenna is attached to the roof of the test vehicle to measure the actual vehicle speed in road tests. And the measurement accuracy of the GPS is about 0.1km/h.

FIGURE 7. Winter test site.

A. STRAIGHT-LINE DRIVING LIMIT CONDITION TEST

In order to fully verify the applicability of the algorithm to different working conditions, especially poor and complex working conditions, emergency braking on the ice road and full throttle accelerations on the ice-asphalt split road are firstly carried out. In the two selected working conditions, the wheel force changes extremely dramatically and the wheel speed fluctuates greatly. Meanwhile, the wheel speed always deviates from the actual vehicle speed, so it is difficult to estimate the reference speed accurately and the change of wheel speed credibility has certain characteristics.

Under emergency braking conditions, the wheels tend to lock up due to the low adhesion coefficient on the ice surface. The ABS function intervenes to regulate the pressure of each wheel cylinder, and the wheel speed alternately fluctuates, as shown in Fig.8. Comparing the reference speed with the actual vehicle speed in Fig. 9, the maximum error is about 0.676m/s, the average error is −0.049m/s, and the estimated value varies relatively smoothly. It should be noted that ABS function requires accurate reference speed as input

to calculate the actual wheel slip rate as control parameter. The accuracy and stability of the reference speed estimation will affect the control effect of ABS function, and then affect the change of wheel speed, which in turn will affect the vehicle speed estimation. Therefore, the accuracy, stability and real-time performance of reference speed estimation results are very important. Figure 10 shows the change in wheel speed credibility, which shows the wheel speed credibility of rear axle is higher than that of front axle. Because the ABS function requires the rear axle to have a lower slip rate than the front axle, and due to axle load transfer, the change of rear axle wheel braking force is relatively small, so the rear axle wheels are more 'stable', which also proves that the wheel speed credibility based on multi-dimensional information comprehensive evaluation can accurately represent the actual stable state of wheels.

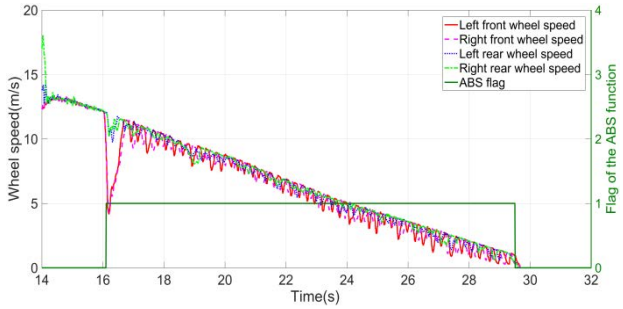

FIGURE 8. Change of wheel speed during emergency braking on ice.

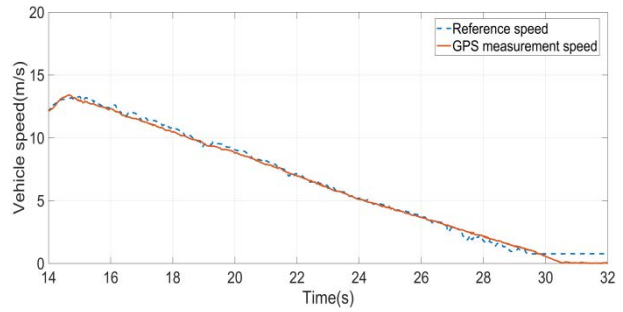

FIGURE 9. Comparison of reference speed and actual vehicle speed by GPS during emergency braking on ice.

Fig. 11-13 show the curves of wheel speed, vehicle speed and wheel speed credibility under full-throttle acceleration on the ice-asphalt split road. As the right wheels are on the ice and the adhesion coefficient is low, the wheels slip in the case of rapidly accelerate. The ASR (Acceleration Slip Regulation) function can control wheel speed on the low adhesion road by adjusting the engine torque and wheel braking force, so that the right wheels slip rate fluctuates within a certain range. Therefore, due to the relatively high slip rate and the continuous large variation in wheel force, the wheel speed credibility on the right side is significantly low. Correspondingly, as the maximum longitudinal force provided by the road with high adhesion coefficient is large,

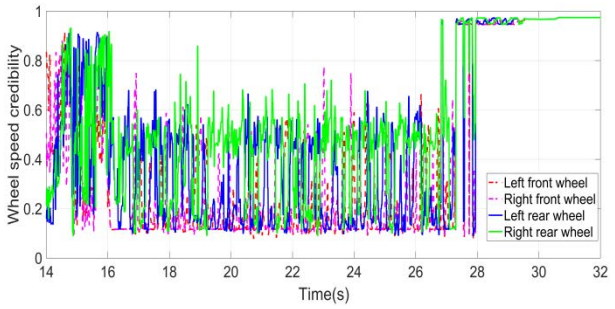

FIGURE 10. Change of wheel speed credibility during emergency braking on ice.

wheels don't slip significantly, so the wheel speed credibility of the two wheels on the left side is high. Meanwhile, the driving torque of the rear axle is larger, the wheel speed credibility of the left rear wheel is slightly lower than left front wheel. The trend of wheel speed credibility and the fluctuation state of the actual wheel speed are generally consistent with the expectation, which proves once again that the fuzzy rules designed for evaluating wheel stable state through multi-information fusion are correct. Due to the existence of higher wheel speed credibility, the final calculated reference speed is highly consistent with the actual speed measured by GPS. The maximum estimation error is about 0.190m/s and the average error is 0.042m/s.

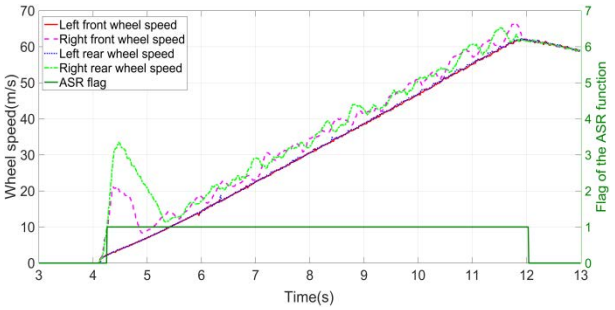

FIGURE 11. Change of wheel speed on the ice-asphalt split road.

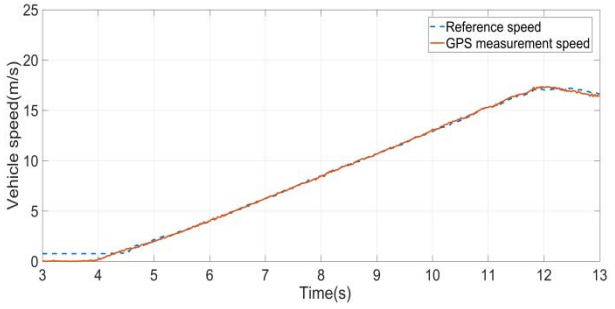

FIGURE 12. Comparison of reference speed and actual vehicle speed by GPS for rapid acceleration on the ice-asphalt split road.

B. STEERING DRIVING LIMIT CONDITION TEST

The VDC (Vehicle Dynamics Control) function intervenes when the vehicle is under extreme steering conditions by

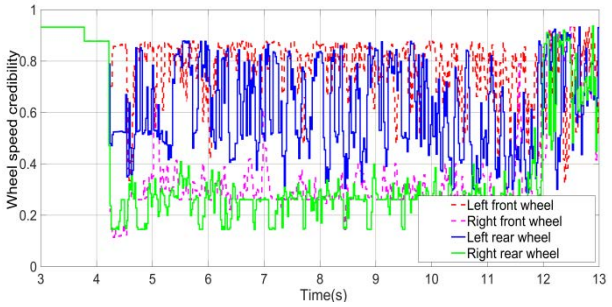

FIGURE 13. Change of wheel speed credibility for rapid acceleration on the ice-asphalt split road.

actively booster braking certain wheels to ensure that the vehicle can follow the driver's desired trajectory and maintain the attitude of the vehicle. Fig. 14 shows the changes of each wheel speed under the intervention of VDC function when the vehicle continuously steers on the compacted snow road. It can be seen that due to the complex working conditions of steering, wheel slip and active pressurization, each wheel speed changes dramatically. Fig. 15 shows the change of wheel speed credibility for each wheel. When the wheel speed fluctuates greatly, the corresponding wheel speed credibility decreases significantly. Vehicle tend to understeer due to low adhesion coefficient. At this time, the VDC function mainly adjusts the vehicle dynamics state by braking the inner rear wheel, so the force of rear axle wheels changes more greatly and credibility is relatively low, which is consistent with the actual situation.

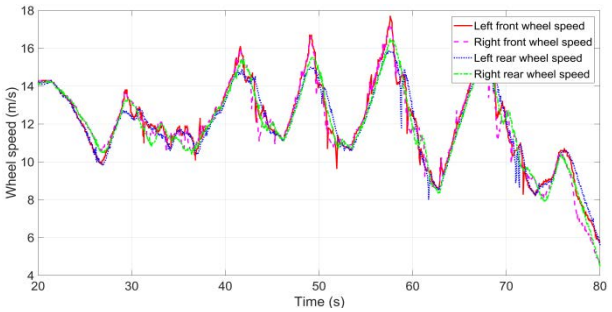

FIGURE 14. Change of wheel speed during VDC function intervention.

Comparing estimated the reference speed with the actual vehicle speed by GPS, as shown in Fig. 16, the maximum error is about 0.482m/s and the average error is 0.051m/s. It can be seen that the reference speed can still accurately and stably describe the actual vehicle speed when the VDC function is enabled and the vehicle is under the extreme sideslip and roll condition.

Fig. 17 shows the change of longitudinal acceleration. Since the estimated reference speed curve is relatively smooth, the acceleration obtained by its differential has a small fluctuation. But the estimated longitudinal acceleration and the acceleration sensor signals have a relatively large fluctuation, the overall trend of the three is basically the

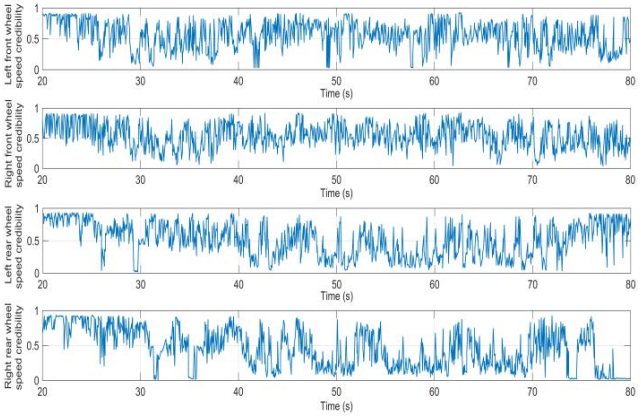

FIGURE 15. Wheel speed credibility during VDC function intervention.

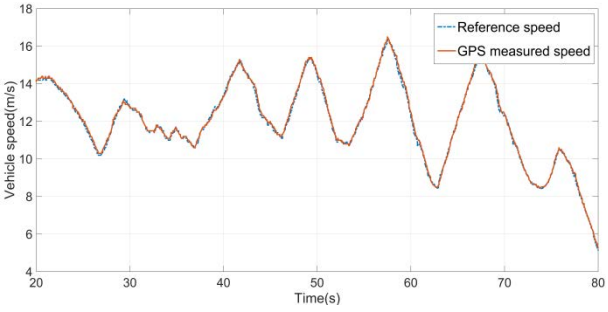

FIGURE 16. Comparison of reference speed and actual speed by GPS.

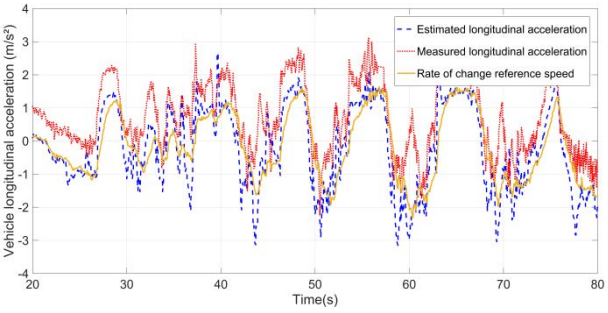

FIGURE 17. Change of longitudinal acceleration.

same. There are some deviations between the acceleration sensor signal and the estimated longitudinal acceleration signal. On the one hand, the measured value of the acceleration contains the lateral acceleration component due to the sideslip angle in the steering process. On the other hand, it may be that the road is not strictly horizontal or the vehicle body has pitch changes, making the measurement value contains other influencing factors.

The Table 3 reflects the deviation between the estimated reference speed and the actual measured value in the road test. Both the maximum and average value of the estimated error are small under the three representative test conditions, with the maximum error less than 0.68m/s, which proves that the algorithm has a high estimation accuracy and adaptability.

Meanwhile, the standard error does not exceed 0.207m/s, which indirectly reflects the high stability real-time performance of the estimated value.

TABLE 3. Estimated errors from vehicle road tests.

Test conditions	Maximum deviation (m/s)	Average deviation (m/s)	Standard deviation (m/s)
Emergency braking on ice road	0.676	-0.049	0.207
Rapid acceleration on the split road	0.190	0.042	0.114
Rapid steering on compacted snow	0.480	0.051	0.122

V. VEHICLE MASS AND SLOPE TESTS VALIDATION

Conventional urban roads and standard slope of the test site are selected to verify the vehicle mass and road slope estimates respectively. The relevant parameters of the test vehicle are shown in Table 4.

TABLE 4. Table of vehicle parameters.

Name	Values	Name	Values
Unladen weight /kg	2308	Distance from rear axle to center of mass /m	1.496
Actual mass /kg	2617	Axlebase /m	2.930
Wheel radius /m	0.371	Wheelbase /m	1.664
Height of mass /m	0.652	Mechanical efficiency	0.9

As for the mass estimation algorithm, considering that the relevant input signals are accurate and stable after the multi-dimensional information is adopted to screen the vehicle state and the vehicle mass is a slow changing value. Therefore, the forgetting factor is set as 1.01, in order to enhance the influence of historical data and ensure the stability of the estimation system. Similarly, for slope estimation, the process noise covariance matrix Q and measurement noise covariance matrix R can be set to smaller values. Because the relevant input signals, including reference speed and sensor signals, can maintain high accuracy and stability in the dynamic environment.

A. CONVENTIONAL URBAN ROADS VALIDATION

In order to obtain the convergence mass several times during a period of driving, the threshold of parking time for restart estimation is adjusted to 5s. And the threshold of covariance of mass estimation convergence is set as 0.0015.

A section of conventional urban road is selected for the tests, and the driver controls the vehicle according to the actual road conditions. Fig. 18 shows the comparison between the reference speed and the speed measured by GPS. Under ordinary urban road conditions, the vehicle is basically in a steady state with no active function involved. In this case, it is relatively easy to estimate the reference speed. When the vehicle is parked, the timer starts, in order to reset the mass estimation algorithm after the estimation results converges.

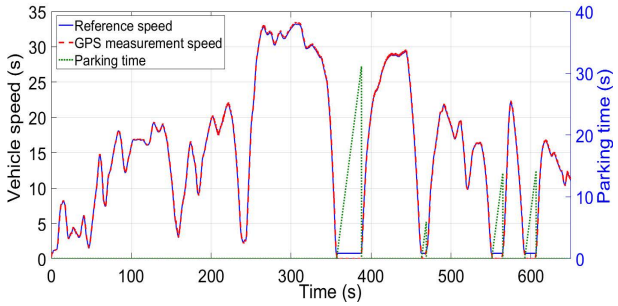

FIGURE 18. Change of vehicle speed under steady state condition.

For the proposed vehicle mass estimation confidence factor based on multi-dimensional information, its change is shown in Fig. 19. When the confidence factor is lower than 0.6, it indicates that the state of the vehicle is unstable, and the estimation algorithm is suspended to avoid the influence of the unreal signal on the estimation result. The blue line represents the absolute value of the longitudinal acceleration of the vehicle. Since it is conventional driving, the peak acceleration is basically maintained within 0.4g.

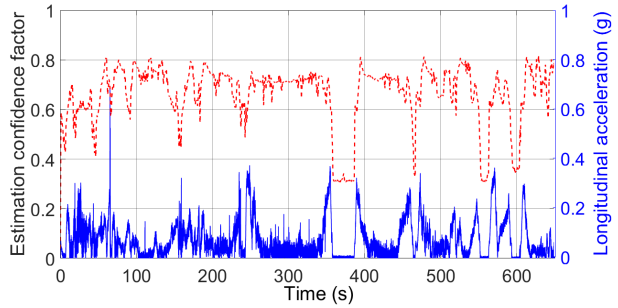

FIGURE 19. Change of mass estimation confidence factor.

The final estimation result is shown in Figure 20, where the blue line is the mass estimate result with the help of RLS. And the green line is the convergence flag, which is determined by using the covariance and the set threshold. Red line is the rough estimation result of the direct division of equivalent driving force and equivalent acceleration, and it fluctuates violently. But the actual result with the highest probability can be effectively extracted by the least square method, so as to obtain the stable output value. The final estimated results are shown in Tab. 5. The maximum relative error between the estimated value and the measured value is less than 1.76%, and the estimation results are close to each other, which verifies the high accuracy and stability of the proposed estimation algorithm. Meanwhile, except for the first time, the convergence time is short. The first estimation is mainly due to the low speed and the confidence factor is lower than the threshold, which led to the suspension of estimation for a long time.

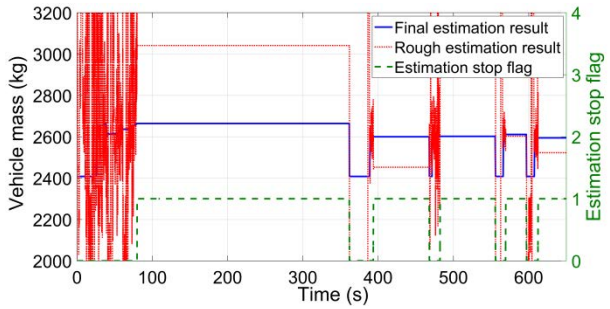

FIGURE 20. Results of mass estimation under steady state condition.

TABLE 5. Mass estimation test results.

	Convergence time/s	Estimation results/kg	Relative error/%
1	53.89	2663	1.76
2	4.50	2599	-0.688
3	10.74	2601	-0.611
4	3.2	2610	-0.267
5	4.78	2594	-0.879

B. STANDARD SLOPE VALIDATION

The road slope tests are carried out on the standard slope in the test site in order to ensure the estimated results can be verified. In the first test, the vehicle speed is maintained at 20-25km/h, and the vehicle pass 10% uphill ramp and 30% downhill ramp respectively. The change of mass estimation is shown in Figure 21, and the initial value is no-load mass. Between 0 and 13.67s, the vehicle is in the process of acceleration and the speed is low, and the confidence factor is lower than the threshold, so the mass estimation is suspended. The final estimation result is 2668kg, the relative error is 1.95%, and the convergence time is 7.13s.

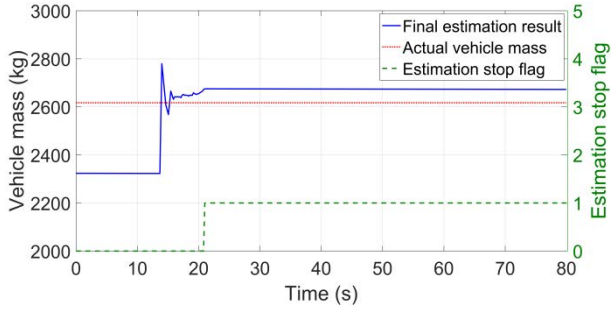

FIGURE 21. Results of mass estimation in the test 1.

Figure 22 shows the change of slope estimation, in which KF estimation result is relatively stable, but there is a certain delay and the absolute error is less than 2.71%. The estimated value of UKF method has better real-time performance, but there is some fluctuation. The final results based on IMM method consider both stability and real-time performance, and the maximum absolute error is less than 1.84%, which has higher accuracy.

In the test 2, the vehicle pass 20% uphill ramp and 10% downhill ramp, and the speed remain between 20 and 25km/h.

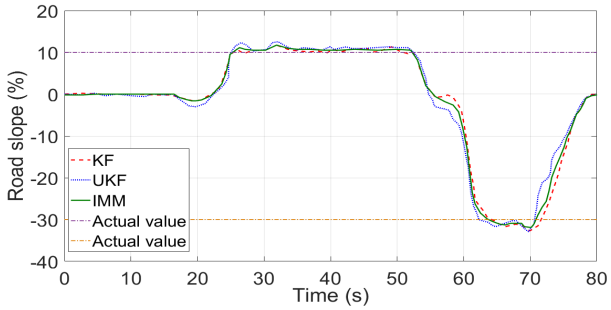

FIGURE 22. Change of road slope estimation in the test 1.

Similar to the results of the test 1, the estimated result based on the KF method changes steadily, but it is small in the uphill phase. And the UKF based estimation has a faster response, but there is a tendency of distortion at some time. Only the estimated value obtained by the interactive multi-model method can be kept near the real slope stably, with the maximum absolute error no more than 1.25%, and the real-time performance can also be guaranteed.

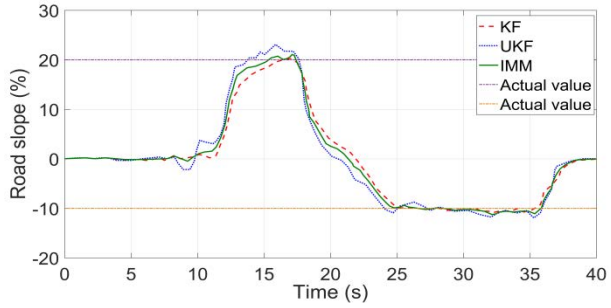

FIGURE 23. Change of road slope estimation in the test 2.

Through the above tests, it is verified that the stable state of the vehicle can be accurately evaluated based on the fusion of the estimated reference speed and other multi-dimensional information. The proposed vehicle mass and road slope estimation algorithm can also achieve accurate and stable estimation under realistic working conditions, which can meet the needs of intelligent vehicles.

VI. CONCLUSION

1) A quantitative representation method of the wheel dynamics stable state based on multi-dimensional information comprehensive evaluation is proposed. On this basis, an algorithm for estimation of reference speed is designed by using wheel speed credibility, which is not limited by working conditions and can achieve accurate estimation in any scenario. Through the typical road tests with difficult estimation, the maximum error between the estimation result and the actual measured value by GPS is less than 0.68m/s, which verifies that the proposed algorithm has high accuracy, stability and real-time performance.

2) Based on high precision reference speed and multi-dimensional information, a calculation method of the vehicle

mass estimation confidence factor based on fuzzy rules is designed, in order to ensure the accuracy of the input state information during the estimation. And then, the mass estimation method based on RLS is proposed. By designing the strategy and fusing the information, the whole algorithm is more suitable for practical application. The maximum relative error is less than 1.95% in relevant road tests.

3) A slope estimation method based on interactive multi-model algorithm is designed to solve the problems caused by kinematics or dynamics estimation alone. Through the tests of standard slope, the IMM based estimation algorithm can give consideration to both stability and real-time performance, and the maximum absolute error is less than 1.84%.

REFERENCES

[1] S. Zhou, H. Zhao, W. Chen, Z. Liu, H. Wang, and Y.-H. Liu, "Dynamic state estimation and control of a heavy tractor–trailers vehicle," *IEEE/ASME Trans. Mechatronics*, vol. 26, no. 3, pp. 1467–1478, Jun. 2021, doi: 10.1109/TMECH.2020.3021705.

[2] J. F. Chen, S. Hu, Y. Ye, H. Huang, R. Langari, and C. Tang, "A cascaded scheme for high-performance estimation of vehicle states," *Proc. Inst. Mech. Eng., D, J. Automobile Eng.*, vol. 235, no. 8, pp. 2101–2113, Jul. 2021, doi: 10.1177/0954407021993240.

[3] L. C. Zhang, A. Weiping, L. Zhibin, Z. Long, and T. Xinmiao, "Stability control of energy saving electric vehicle using dynamic nonlinear system state estimation," *Fractals*, vol. 30, no. 2, pp. 1–12, Jan. 2022, doi: 10.1142/S0218348X22400965.

[4] C. Wang, Z. Wang, L. Zhang, D. Cao, and D. G. Dorrell, "A vehicle rollover evaluation system based on enabling state and parameter estimation," *IEEE Trans. Ind. Informat.*, vol. 17, no. 6, pp. 4003–4013, Jun. 2020, doi: 10.1109/TII.2020.3012003.

[5] L. Q. Jin, D. Tian, Q. Zhang, and J. Wang, "Optimal torque distribution control of multi-axle electric vehicles with in-wheel motors based on DDPG algorithm," *Energies*, vol. 13, no. 6, pp. 1306–1331, Mar. 2020, doi: 10.3390/en13061331.

[6] B. Meng, F. Yang, J. Liu, and Y. Wang, "A survey of brake-by-wire system for intelligent connected electric vehicles," *IEEE Access*, vol. 8, pp. 225424–225436, 2020, doi: 10.1109/ACCESS.2020.3040184.

[7] Y. Lei, J. Luo, X. Song, M. Li, P. Wen, and Z. Xiong, "Robust vehicle speed measurement based on feature information fusion for vehicle multi-characteristic detection," *Entropy*, vol. 23, no. 7, pp. 910–932, Jul. 2021, doi: 10.3390/e23070910.

[8] X. Q. Xiao, "Research on the key technology of driving behavior recognition based on information fusion," Ph.D. dissertation, School Mechanism Automobile Eng., Hefei Univ. Technol., Hefei, China, 2011.

[9] C. Chen, L. Liu, S. Wan, X. Hui, and Q. Pei, "Data dissemination for industry 4.0 applications in Internet of Vehicles based on short-term traffic prediction," *ACM Trans. Internet Technol.*, vol. 22, no. 1, pp. 1–18, Feb. 2022, doi: 10.1145/3430505.

[10] W. Wei, R. Yang, H. Gu, W. Zhao, C. Chen, and S. Wan, "Multi-objective optimization for resource allocation in vehicular cloud computing networks," *IEEE Trans. Intell. Transp. Syst.*, early access, Aug. 3, 2021, doi: 10.1109/TITS.2021.3091321.

[11] V. Markevicius *et al.*, "Analysis of methods for long vehicles speed estimation using anisotropic magneto-resistive (AMR) sensors and reference piezoelectric sensor," *Sensors*, vol. 20, no. 12, pp. 3541–3555, Jun. 2020, doi: 10.3390/s20123541.

[12] C. Pomponi, S. Scalzi, L. Pasquale, C. M. Verrelli, and R. Marino, "Automatic motor speed reference generators for cruise and lateral control of electric vehicles with in-wheel motors," *Control Eng. Pract.*, vol. 79, pp. 126–143, Oct. 2018, doi: 10.1016/j.conengprac.2018.07.008.

[13] J. Li *et al.*, "Sliding mode control of ABS neural network for commercial vehicles based on longitudinal vehicle speed estimation," *J. Jilin Univ. Eng. Technol. Ed.*, vol. 49, no. 4, pp. 1017–1025, Mar. 2020, doi: 10.13229/j.cnki.jdxbgxb20180517.

[14] D. P. Zhang, S. Liangbo, Y. Xuejin, W. Beihai, and W. Luan, "Control method of wheel slip rate based on fuzzy algorithm," *J. Intell. Fuzzy Syst.*, vol. 38, no. 6, pp. 7865–7874, May 2020, doi: 10.3233/JIFS-1798562020.

[15] X. W. Zhang, Y. Xu, M. Pan, and F. Ren, "A vehicle ABS adaptive sliding-mode control algorithm based on the vehicle velocity estimation and tyre/road friction coefficient estimations," *Vehicle Syst. Dyn.*, vol. 52, no. 4, pp. 475–503, Feb. 2020, doi: 10.1080/00423114.2013.864775.

[16] M. Klomp, Y. Gao, and F. Bruzelius, "Longitudinal velocity and road slope estimation in hybrid electric vehicles employing early detection of excessive wheel slip," *Vehicle Syst. Dyn.*, vol. 52, no. 1, pp. 172–188, Jul. 2014, doi: 10.1080/00423114.2014.887737.

[17] B. Zhang *et al.*, "Study on dynamic frequency domain distribution of suspension system under non-smooth random excitation," *Sci. Technol. Eng.*, vol. 17, no. 33, pp. 212–216, Jan. 2018, doi: 10.3969/j.issn.1671-1815.2017.33.031.

[18] Z. Yu *et al.*, "Design of control strategies for improving the maneuverability of distributed drive electric vehicles," *J. Tongji Univ. Natural Sci. Ed.*, vol. 42, no. 7, pp. 1088–1095, Jul. 2014, doi: 10.3969/j.issn.0253-374x.2014.07.016.

[19] J. Song *et al.*, "Differential steering and control based on tyre lateral deflection," *J. Tsinghua Univ. Natural Sci. Ed.*, vol. 60, no. 2, pp. 20–26, Jan. 2020, doi: 10.16511/j.cnki.qhdxxb.2019.22.044.

[20] Z. Ren *et al.*, "Research on lane keeping assist control strategy under visual failure condition," *Automot. Technol.*, vol. 8, pp. 6–13, Aug. 2020, doi: 10.19620/j.cnki.1000-3703.20190498.

[21] F. Lai, C. Q. Huang, and H. L. Dong, "Safety distance model of automatic emergency collision avoidance system for intelligent vehicles and its comparative analysis," *J. Chongqing Univ. Technol. Natural Sci.*, vol. 34, no. 9, pp. 39–46, Sep. 2020, doi: 10.3969/j.issn.1674-8425(z).2020.09.004.

[22] R. Ritschel, F. Schrödel, J. Hädrich, and J. Jäkel, "Nonlinear model predictive path-following control for highly automated driving," *IFAC-Papers OnLine*, vol. 52, no. 8, pp. 350–355, Sep. 2019, doi: 10.1016/j.ifacol.2019.08.112.

[23] K. Hiroki, M. Masakazu, and F. Kensaku, "Vehicle speed estimation by in-vehicle camera," in *Proc. World Automat. Congr. (WAC)*, Puerto Vallarta, Mexico, Jun. 2012, pp. 1–6.

[24] L. R. Costa, M. S. Rauen, and A. B. Fronza, "Car speed estimation based on image scale factor," *Forensic Sci. Int.*, vol. 310, May 2020, Art. no. 110229, doi: 10.1016/j.forsciint.2020.110229.

[25] T.-W. Pai, W.-J. Juang, and L.-J. Wang, "An adaptive windowing prediction algorithm for vehicle speed estimation," in *Proc. IEEE Intell. Transp. Syst. (ITSC)*, Aug. 2001, pp. 901–906, doi: 10.1109/ITSC.2001.948780.

[26] T. F. Xu, "Research on longitudinal speed estimation algorithm for four-wheeled wheel-side drive electric vehicles," M.S. thesis, College Automot. Stud., Tongji Univ., Shanghai, China, 2008.

[27] X. Zhang *et al.*, "A review of key technologies for automotive ABS control systems," *J. Electr. Mech. Eng.*, vol. 26, no. 12, pp. 1–4, Dec. 2009, doi: 10.3969/j.issn.1001-4551.2009.12.001.

[28] L. J. Wu and L. F. Wang, "A reference vehicle speed estimation method based on acceleration and wheel speed information," *Automot. Technol.*, vol. 1, pp. 45–48, Jan. 2011, doi: 10.3969/j.issn.1000-3703.2011.01.010.

[29] T. X. Zheng, F. L. Ma, and K. B. Zhang, "Estimation of reference vehicle speed based on T-S fuzzy model," *Proc. Eng.*, vol. 15, pp. 188–193, Aug. 2011, doi: 10.1016/j.proeng.2011.08.038.

[30] L. Sun, "Key technology research on transverse sway stability control strategy for wheelside drive electric buses based on reference model," M.S. thesis, College Mech. Eng., Southwest Jiaotong Univ., Chengdu, China, 2019.

[31] Z. P. Yu and G. X. Liu, "Research on the calculation method of reference speed during braking of automobiles," *Shanghai Automobile*, vol. 5, pp. 1–3, May 1998.

[32] L. P. Mo, "Predictive control for energy management of plug-in hybrid electric grid-connected vehicles based on roadwork information," M.S. thesis, College Mech. Eng. Automat., Fuzhou Univ., Fuzhou, China, 2018.

[33] Y. Li *et al.*, "A multi-sensor information fusion approach for vehicle speed estimation," *J. Jiangsu Univ. Natural Sci. Ed.*, vol. 28, no. 4, pp. 301–304, Apr. 2007, doi: j.issn.1671-7775.2007.04.007.

[34] X. Ding, Z. Wang, L. Zhang, and C. Wang, "Longitudinal vehicle speed estimation for four-wheel-independently-actuated electric vehicles based on multi-sensor fusion," *IEEE Trans. Veh. Technol.*, vol. 69, no. 11, pp. 12797–12806, Nov. 2020, doi: 10.1109/TVT.2020.3026106.

[35] W. Cheng, S. Chuanxue, and L. Jianhua, "Research on key state parameters estimation of electric vehicle ESP based on multi-sensor," in *Proc. 5th Int. Conf. Instrum. Meas., Comput., Commun. Control (IMCCC)*, Sep. 2015, pp. 29–32, doi: 10.1109/IMCCC.2015.13.

[36] J. Yu, H. Zhu, H. Han, Y. J. Chen, J. Yang, Y. Zhu, Z. Chen, G. Xue, and M. Li, "SenSpeed: Sensing driving conditions to estimate vehicle speed in urban environments," *IEEE Trans. Mobile Comput.*, vol. 15, no. 1, pp. 202–216, Jan. 2016, doi: 10.1109/TMC.2015.2411270.
[37] C. H. Chen, C. Lee, and C. Lo, "Vehicle localization and velocity estimation based on mobile phone sensing," *IEEE Access*, vol. 4, pp. 803–817, 2016, doi: 10.1109/ACCESS.2016.2530806.
[38] M. Tanelli, S. Savaresi, and C. Cantoni, "Longitudinal vehicle speed estimation for traction and braking control systems," in *Proc. 8th Int. Conf. Intell. Syst. Design Appl.*, Munich, Germany, 2006, pp. 2790–2795, doi: 10.1109/CACSD-CCA-ISIC.2006.4777080.
[39] L. Kong *et al.*, "Method of calculating vehicle reference speed for ABS of off-road vehicle," *Trans. Chin. Soc. Agricult. Machinery*, vol. 37, no. 7, pp. 19–22, Jul. 2006, doi: 110.3969/j.issn.1000-1298.2006.07.005.
[40] R. J. Mau and P. J. Venhovens, "Parametric vehicle mass estimation for optimisation," *Int. J. Vehicle Des.*, vol. 72, no. 1, pp. 1–16, Jan. 2016, doi: 10.1504/IJVD.2016.079202.
[41] W. B. Chu, Y. Lu, J. Lu, and K. Li, "Vehicle mass and road slope estimates for electric vehicle," *Tsinghua Univ. Sci. Technol.*, vol. 54, no. 6, pp. 724–728, Jun. 2014, doi: 10.16511/j.cnki.qhdxxb.2014.06.010.
[42] A. Vahidi, A. Stefanopoulou, and H. Peng, "Recursive least squares with forgetting for online estimation of vehicle mass and road grade: Theory and experiments," *Vehicle Syst. Dyn.*, vol. 43, no. 1, pp. 31–55, Jan. 2005, doi: 10.1080/00423110412331290446.
[43] H. Ling and B. Huang, "Research on torque distribution of four-wheel independent drive off-road vehicle based on PRLS road slope estimation," *Math. Problems Eng.*, vol. 2021, pp. 1–11, Sep. 2021, doi: 10.1155/2021/5399588.
[44] S. Q. Hao, P. P. Luo, and J. Q. Xi, "Estimation of vehicle mass and road slope based on steady-state Kalman filter," in *Proc. IEEE Int. Conf. Unmanned Syst. (ICUS)*, Beijing, China, Feb. 2018, pp. 582–587, doi: 10.1109/ICUS.2017.8278412.
[45] M. Bykkpr and E. Uzunsoy, "Reliability of extended Kalman filtering technic on vehicle mass estimation," *J. Innov. Sci. Eng.*, vol. 5, no. 1, pp. 1–11, Jun. 2021, doi: 10.38088/jise.755616.
[46] B. Y. Li, J. Zhang, H. Du, and W. Li, "Two-layer structure based adaptive estimation for vehicle mass and road slope under longitudinal motion," *Measurement*, vol. 95, pp. 439–455, Jan. 2017, doi: 10.1016/j.measurement.2016.10.045.
[47] P. Sahlholm and K. H. Johansson, "Road grade estimation for look-ahead vehicle control using multiple measurement runs," *Control Eng. Pract.*, vol. 18, no. 11, pp. 1328–1341, Nov. 2010, doi: 10.1016/j.conengprac.2009.09.007.
[48] H. S. Bae, J. Ryu, and J. C. Gerdes, "Road grade and vehicle parameter estimation for longitudinal control using GPS," in *Proc. IEEE Conf. Intell. Transp. Syst.*, Oakland, CA, USA, Jan. 2001, pp. 25–29.
[49] J. Zhao, L. Zhi-xuan, Z. Bing, L. Ya-xin, and S. Yu-ze, "Vehicle mass and road slope estimation based on interactive muli-model," *China J. Highway Transp.*, vol. 32, no. 12, pp. 58–65, Nov. 2019, doi: 10.19721/j.cnki.1001-7372.2019.12.006.
[50] X. Fu *et al.*, "UKF estimation of state parameters of four wheel independent drive vehicle," *J. Wuhan Univ. Technol., Transp. Sci. Eng.*, vol. 41, no. 3, pp. 379–384, Mar. 2017, doi: 10.3963/j.issn.2095-3844.2017.03.004.
[51] J. X. Zhang and J. Li, "Vehicle state estimation based on interactive multiple model and cubature Kalman filter," *Automot. Eng.*, vol. 39, no. 9, pp. 977–983, Sep. 2017, doi: 10.19562/j.chinasae.qcgc.2017.09.001.
[52] H. Wilmar, "Improving the response of a wheel speed sensor by using a RLS lattice algorithm," *Sensors*, vol. 6, no. 2, pp. 64–79, Feb. 2006, doi: 10.3390/s6020064.
[53] F. Zhao *et al.*, "Research on vehicle wheel speed recognition algorithm," *Agricult. Equip. Vehicle Eng.*, vol. 58, no. 9, pp. 67–71, Sep. 2020, doi: 10.3969/j.issn.1673-3142.2020.09.016.
[54] P. Li, J. Song, and L. Y. Yu, "Pre-processing algorithm for wheel speed signal rejection in automotive anti-lock braking system," *Road Traffic Technol.*, vol. 18, no. 4, pp. 120–132, Apr. 2001, doi: 10.3969/j.issn.1002-0268.2001.04.033.

DUANYANG TIAN was born in Liaoning, China, in 1993. He received the B.E. degree in mechanical design, manufacture, and automation from Beijing Forestry University, Beijing, China, in 2016, and the M.E. degree in automotive engineering from Jilin University, Jilin, China, in 2019, where he is currently pursuing the Ph.D. degree with the State Key Laboratory of Automotive Simulation and Control, College of Automotive Engineering.

His research interests include the dynamics control of electric vehicles and deep reinforcement learning.

LIQIANG JIN received the B.E. degree in automotive engineering from the Hebei University of Technology, China, and the Ph.D. degree in automotive engineering from Jilin University, Jilin, China, in 2006.

He was hired as a Professor and the Doctoral Supervisor, in 2011. His research interests include the dynamics control of electric vehicles and automotive chassis system design and control.

ZHIHUI ZHANG received the Ph.D. degree in material processing from Jilin University, Jilin, China, in 2007. In 2014, he was conducted a visiting research at The University of Manchester, U.K. He is currently a Professor and the Doctoral Supervisor. He was awarded the National Science Foundation for Distinguished Young Scholars, in 2020.

HAO LI was born in Bozhou, Anhui, China. He received the Engineering degree from the Department of Vehicle Engineering, Xi'an University of Science and Technology, in 2020. He is currently pursuing the master's degree with the School of Automotive Engineering, Jilin University. His research interest includes the dynamics and control of electric vehicles.